Species Distribution within the Soluble Phase beyond the Gel Point

Dimitris S. Argyropoulos,* Richard M. Berry, and Henry I. Bolker

Pulp and Paper Research Institute of Canada, Pointe Claire, P.Q., Canada H9R 3J9, and Department of Chemistry, McGill University, Montreal, P.Q., Canada H3A 2A7.
Received July 30, 1986

ABSTRACT: An equation describing the species distribution during the copolymerization of *f*-functional monomers with difunctional monomers has been derived based on known relationships. The formation of network polymerization sols isolated over the entire region beyond the gel point was followed, and their distributions were characterized by quantitative gel permeation chromatography coupled with low-angle laser light scattering. The critical point is represented as a turning point for the overall species distribution. Beyond the gel point the development of molecular weight distribution of the isolated sols is shown to follow a reverse path to that of gelation up to the gel point. Accordingly, the first and second solutions of the distribution equation derived gave a fair fit with the experimental results. Beyond the gel point, however, the physical state of the system does not allow the system to be amenable to a fully stochastic reaction pathway as in the region before the critical point. As a result the solution of the equations for pentadecamers showed serious discrepancies with the experiments. The magnitude of the discrepancies was found to progressively increase with increasing conversion beyond the gel point.

Introduction

As polymerization advances during gelation, larger polymers are produced by the gradual consumption of smaller species. At the same time, the overall species distribution becomes increasingly broader, with maximum heterogeneity at the critical point, where an infinite network abruptly appears. Beyond the gel point the soluble fraction and the molecular weight averages that characterize it gradually decrease. This effect is thought to occur by species of higher complexity becoming preferentially attached to the gel. The network thus grows at the expense of the larger species. Flory[1] has pointed out that beyond the gel point the molecular species distribution of the sol fraction will "undergo retroversion over the course followed up to the gel point". Such a qualitative description of the process forms the theoretical foundations of all gelation theories. Gordon and his team[2-4] have confirmed the validity of this description up to the gel point and just beyond it. The expected retroversion of the sol's molecular properties is too important a phenomenon to ignore. This paper therefore attempts to answer each of the following questions:

1. Does retroversion of species distribution take place as polymerization proceeds further beyond the gel point?
2. Do the various solutions of a weight fraction distribution equation (monomers, dimers, etc.) quantitatively fit the experimental results beyond the gel point?
3. Are the soluble species of higher functionality preferentially included in the gel phase as polymerization advances toward completion?
4. How does diffusion affect the overall species distribution and the network-building process?

These questions were addressed by conducting the stoichiometric polycondensation of 1,3,5-benzenetriacetic acid with 1,10-decamethylene glycol (BTA/DMG), isolating the soluble fractions at various stages beyond the gel point, and characterizing them by quantitative gel permeation chromatography and low-angle laser light scattering photometry (GPC/LALLS).

Results and Discussion

Species Distribution during Polymerization. Clarke, Devoy, and Gordon[4] have reported on the quantitative GPC of samples taken from the BTA/DMG polymerization up to about 65% conversion (gel point 70.7%). The resolution of their chromatograms revealed that the weight fraction of both monomers and dimers was in accord with the random polymerization scheme. With a similar GPC instrument and a set of high-performance columns (μStyragel) having an exclusion limit greater than 10×10^6 molecular weight, sol samples isolated from the BTA/DMG gelation gave the chromatograms of Figure 1. Here, however, the chromatograms represented the species distribution over the entire region beyond the gel point. The similarity of their shapes to the shapes of those reported by Clarke et al. is striking, although the latter had a somewhat better peak resolution. (Unfortunately, no details of their chromatographic setup were reported.)

These distributions exhibit three primary features: (i) Each sol fraction shows a broad distribution with reasonable resolution of the low molecular weight species. (ii) The breadth of the distributions increases nearer the gel point. As the polymerization proceeds, the high molecular weight tail vanishes, qualitatively indicating that the network grows at the expense of high molecular weight species. (iii) The DMG peak, which represents the difunctional monomer, appears to grow as the polymerization proceeds toward completion. This last feature is in complete agreement with Berry's[5] prediction that DMG is the surviving species at the limiting value of p, i.e., $p \rightarrow 1.0$ (where p is the extent of reaction, or conversion).

These observations are most telling arguments for the essentially identical form of distribution in pregel and postgel samples.

From Falk and Thomas'[6] conclusions regarding the applicability of Stockmayer's[7,8] distribution expression (1), one could proceed to correlate theoretical weight fraction predictions with the results obtained from the chromatograms of Figure 1 in order to determine whether the retroversion affect is quantitative.

$$W_x = \left\{ \frac{(fx - x)!f}{(x - 1)!(fx - 2x + 2)!} \right\} \alpha^{x-1}(1 - \alpha)^{fx-2x+2} \quad (1)$$

where α is the branching coefficient, f is the average monomer functionality, x is the number of units in an x-mer, and W_x is the weight fraction of any x-mer.

A point, however, of major criticism in such an operation could be the fact that eq 1 was originally derived by Stockmayer so as to describe the f-functional random

*Author to whom correspondence should be addressed at the Pulp and Paper Research Institute of Canada.

0024-9297/87/2220-0357$01.50/0

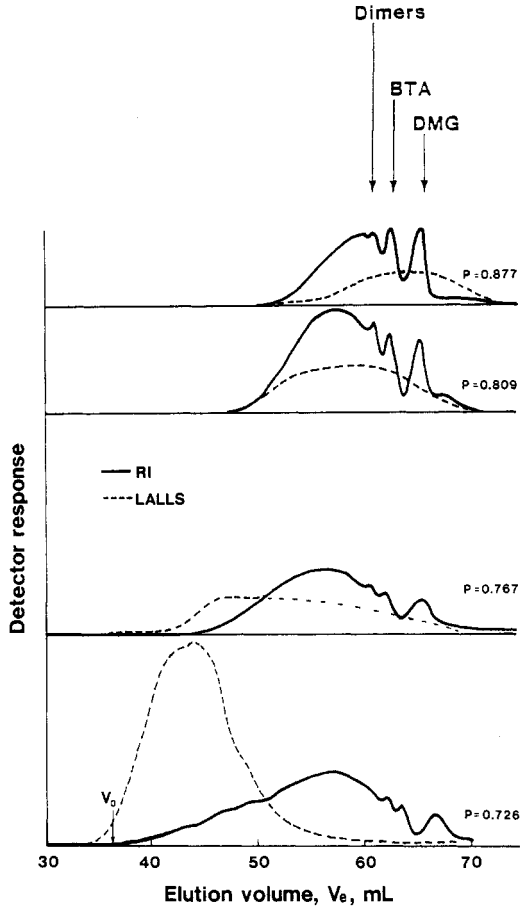

Figure 1. GPC/LALLS combined outputs for BTA/DMG polymerization sols beyond the gel point: (—) response of differential refractometer; (– – –) response of the LALLS photometer. Peak assignment according to Clarke et al.[4] p is the extent of reaction.

polymerization and not the copolymerization of multifunctional monomers, which is the case in question.

The various relationships necessary for deriving a distribution equation for such a case were worked out by Stockmayer in 1943.[7] It thus became possible to derive an equation specific for our experiments.

$$W_x = \left\{\left(\frac{2^s f^n (fn-n)!s!}{[(fn-n-s+1)]!(s-n+1)!}\left[\frac{pr(1-p)^{f-1}}{f(1-rp)}\right]^n \times \left[\frac{p(1-rp)}{2(1-p)}\right]^s\right)/(n!s!)\right\}(n+s) \times \left\{\frac{[(1-p)+p(1-rp)]^2\alpha}{p(1-rp)(1-p)f(1-\alpha)^2} + \frac{p(1-rp)}{2(1-p)}\left[\frac{[(1-p)+p(1-rp)]\alpha}{p(1-rp)(1-\alpha)}+1\right]^2\right\}^{-1} \quad (2)$$

where $W_x = W_{n,s}$ is the weight fraction of n,s-mer, α is the branching probability ($\alpha = p^2$ for the BTA/DMG case), p is the extent of reaction, n is the number of trifunctional molecules per x-mer, s is the number of difunctional molecules per x-mer, r is the stoichiometric ratio of monomers, and f is the functionality of the polyfunctional monomer. The algebra and substitutions required so as to arrive at expression 2 are shown in the Appendix.

Figure 2 shows the evaluation of eq 2 for the two monomers and dimers over the entire course of the polymerization. For $r = 1$ and at the limiting value of $p = 0$ the

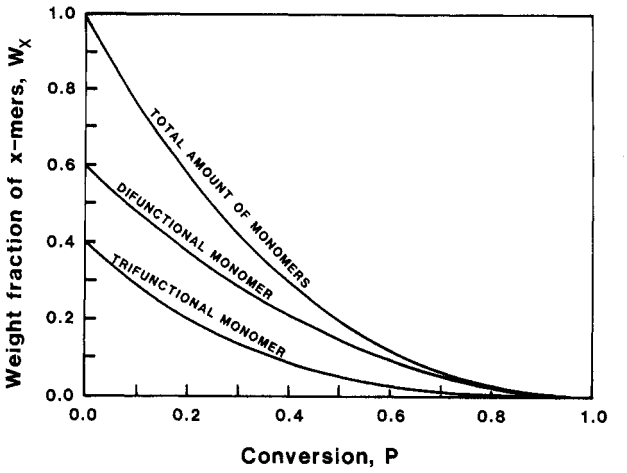

Figure 2. Theoretical plots describing the consumption of two monomers during their stoichiometric copolymerization, i.e., a trifunctional with a difunctional. The plots are derived from eq 2 by setting $f = 3$, $r = 1$, $\alpha = p^2$, $n = 0$, and $s = 1$ for difunctional and $f = 3$, $r = 1$, $\alpha = p^2$, $n = 1$, and $s = 0$ for trifunctional monomers. The total monomer curve is the result of adding the monomer compositions at each conversion value.

equation correctly predicts the weight fractions of difunctional and trifunctional monomers to be 0.6 and 0.4, respectively.

Thus, it became possible to compare the results of eq 2 with those of the Stockmayer expression (1) when the latter was approximated to describe the BTA/DMG system by setting $f = 2.5$ and $\alpha = p$. The results of this comparison showed that virtually identical figures are obtained for monomers and dimers over the entire course of the polymerization. For higher members of the series, however, the approximation introduces significant errors.

Beyond the gel point a calculated value of W_x receives physical significance when divided by the theoretical weight of sol fraction (W_s) present at a particular degree of reaction. The relationship that quantifies W_s for such a copolymerization is as follows:

$$W_s = M_{A_f}P(F_A{}^{out})^3 + M_{B_2}(3/2)P(F_B{}^{out})^2 - M_c(3p)P(F_A{}^{out})^2P(F_B{}^{out})/[M_{A_f} + M_{B_2}(3/2) - M_c(3p)] \quad (3)$$

where $P(F_A{}^{out}) = (1-p^2)/p^2$ and $P(F_B{}^{out}) = [P(F_A{}^{out}) - 1 + p]/p$. M_c is the molecular weight of the condensation product, and M_{B_2} and M_{A_f} are the molecular weights of the difunctional and polyfunctional monomers, respectively.

This has been specifically derived[5] for the f-functional/difunctional copolymerization based on the recursive approach of Macosko and Miller.[9] It has also been tested experimentally in the region beyond the gel point for a variety of copolymerization systems with adequate success.[10]

Thus by calculating the theoretical weight fractions for $W_{x=1}$ and $W_{x=2}$ at various stages beyond the gel point from eq 2 and then dividing with their theoretical W_s counterparts derived from eq 3, we derived the theoretical plots of Figure 3 beyond the gel point.

The chromatograms of Figure 1 showed sufficient resolution of the lowest members of the series that their weight fractions could quantitatively be determined. Similar chromatographic information in two papers,[4,11] together with test runs in this laboratory on pure compounds, permitted peak assignments to be made with confidence. The weight fractions of the two monomers and the dimer, as determined by repeated cut and weigh measurements, are also shown in Figure 3, where the

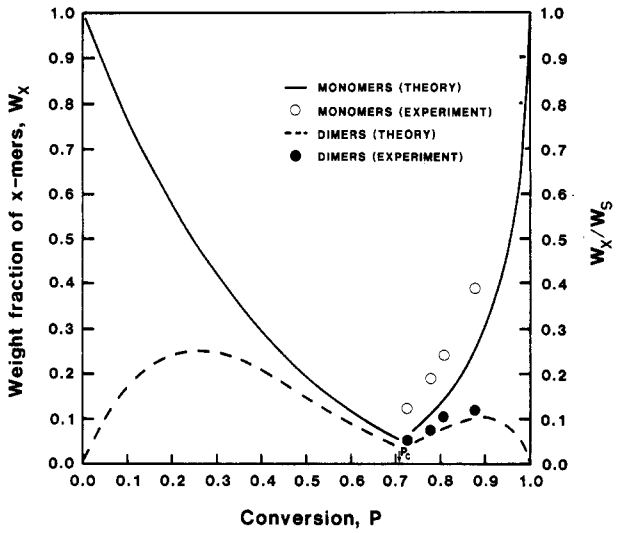

Figure 3. Theoretical plots of eq 2 for total monomers and dimers. Beyond the gel point the plots are reversed as calculated according to the procedure discussed in the text. For comparison, the experimental values of W_x/W_s for $x = 1$ and $x = 2$ are also shown.

combined weight fractions of the two monomers and that of the dimer are plotted. The experimentally determined monomer weight fractions at various stages of the polycondensation beyond the gel point qualitatively follow the path defined by the theoretical curve. A quantitative agreement was obtained for the $W_{x=2}$ (dimers) weight fractions. Even the shape of the experimental curve is very similar to the theoretical curve, at least up to $p = 0.877$. These results support the theory, at least qualitatively.

The computer-interfaced GPC/LALLS photometer, marketed by Chromatix Inc. (Sunnyvale, CA), provides an interesting option for data display:[12] a plot of species weight fraction vs. its molecular weight. This plot effectively represents valuable polymer fractionation data. The accuracy of such a fractionation technique was examined with a series of low molecular weight monodisperse polystyrenes with adequate success and reproducibility. The sol fractions of BTA/DMG isolated at 0.726, 0.767, and 0.877 conversion values were injected into the photometer, with the results shown in Figure 4. Quantitatively, however, these results represented only the weight fractions of the species that possess molecular weights above (3–5) $\times 10^3$, totally excluding all other oligomers. Such an arbitrary exclusion of the low molecular weight species could introduce serious errors in any subsequent calculations and in turn might lead to doubtful conclusions. The results of Figure 4 seem to be representative of only the light-scattering active species.

Table I
Approximate Weight Fractions of Pentadecamer in Sol Samples Obtained from the Polymerization of BTA/DMG, Theoretical Values, and the Ratio of Experiment to Theory Showing the Trend of the Discrepancy

	theory			expt	expt/theory
conversion	W_s[a]	$W_{x=15}$[b]	$W_{x=15}/W_s$	$W_{x=15}/W_s$[c]	(col 5)/(col 4)
0.726	0.733	0.0115	0.0157	0.021	1.3
0.767	0.357	0.0066	0.0185	0.159	8.6
0.877	0.037	0.00025	0.0068	0.070	10.3

[a] Calculated from eq 3 by setting $M_{A_f} = 252$ and $M_{B_2} = 174$. [b] Calculated from eq 2 for its four nonisomeric forms (see Appendix). [c] Determined from the chromatograms of Figure 1.

This deficiency may be overcome, however, if the data in Figure 4 are coupled with those in Figure 1. Figure 1 gives the molecular weight cutoff information, because it simultaneously displays the light-scattering response for each increment of the GPC curve (RI response). Since the RI detector responds linearly to refractive index differences, its response is a function of concentration. The LALLS detector responds linearly to the scattering intensity, which is a function of concentration and molecular weight. Thus, the sol sample at $p = 0.726$ contained only 39% of light-scattering active species (as derived by cutting and weighing the chromatogram). By multiplying the W_x data of Figure 4 for $p = 0.726$ by this factor, one can approximately determine the real weight fraction of some species in this sol sample. This is not possible, however, for the sols at $p = 0.767$ and $p = 0.877$, because the light-scattering information of Figure 1 for these samples was not as resolvable as for the sample at $p = 0.726$. Instead, one can assume that the monomers and dimers were light-scattering inactive, because they possess the lowest molecular weights. Their combined weight fractions, however, are given in Figure 3. Their contributions could thus be calculated so as to provide the approximate weight fraction of each resolved species in Figure 4.

Such calculations were possible for the sol samples of Figure 4. The pentadecamer peak (15-mer, $x = 15$) was adequately resolved in all three chromatograms. Accordingly, the fractionation data for this particular species were used to examine the validity of eq 2 for its 15th solution beyond the gel point (Table I). A point of criticism that can be made in relation to the accuracy of the $W_{x=15}$ values thus determined is that one does not know if within the peaks taken to represent the pentadecamer all its isomeric and nonisomeric forms are included. It is, however, reasonable to assume that due to their highly branched nature the various forms of this species will not possess entirely different hydrodynamic volumes, causing them to elute at

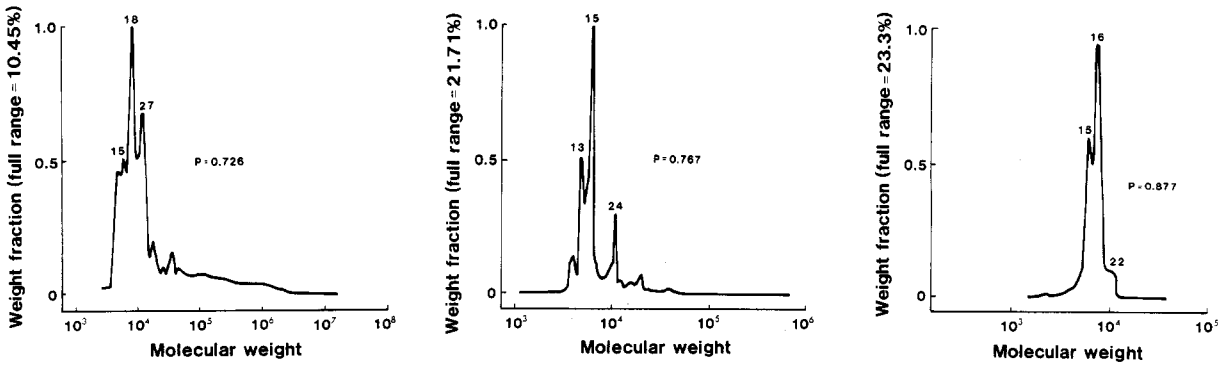

Figure 4. Fractionation curves obtained by the GPC/LALLS of sols isolated beyond the gel point during the polymerization of BTA/DMG. The numbers on the peaks indicate the degree of polymerization of the resolved species (molecular weight per repeating unit = 459).

different stages during the size exclusion process. Due to all the above errors and limitations the values of $W_{x=15}$ thus determined are characterized as "approximate". They are, however, of sufficient accuracy to, at least qualitatively, test the theory.

According to Table I, the pentadecamer content in the sol fraction isolated just after the gel point ($p = 0.726$) was approximately 2.1% (w/w), while the theoretically estimated value is 1.57% (w/w). Although the experimental value was about 1.3 times higher than the theoretical value, the agreement can be taken as reasonable if one considers the errors and limitations of the technique used to determine such an ordinarily inaccessible quantity. A better agreement between theory and experiment is probably unrealistic to expect considering the various deviations from ideality in the region beyond the gel point.

The common assumptions among theories of gelation are the absence of intramolecular cyclization and that molecular reactivities and mobilities are not affected by the previous history of the reacting system. For the BTA/DMG polycondensates, the cyclization effect is small, though definitely measurable.[13,14] Previous experimental data from our laboratory[15] suggest that the ratio of intramolecular to intermolecular reaction actually increases as the reaction proceeds beyond the gel point. This will cause the measured values of p to be increasingly higher than what they should have been if cyclization did not operate. Furthermore, the two sets of values could hardly be expected to be closer if diffusion, which was found to operate beyond the gel point,[16] is also taken into consideration. The pentadecamer contents of the sols at $p = 0.767$ and $p = 0.877$ were approximately 8 and 10 times higher, respectively, than their theoretical estimates. The higher the conversion beyond the gel point, the greater the discrepancy. It has been found[15] that much beyond the gel point the molecular weights of the sol fractions were somewhat higher than those predicted by the theory. Polymer entrapment within the rigid framework of the gel was suggested as accounting for these discrepancies. The increased differences in pentadecamer contents provide additional evidence of polymer entrapment. Since the diffusion effect together with polymer entrapment seriously violates the theoretical assumption of random bond formation within the growing network, the mathematical theory seems to break down much beyond the gel point. The effects of these factors are further demonstrated in this attempt to apply the distribution expression to the pentadecamer.

Diffusion does not operate before the gel point,[17] nor is polymer entrapment possible there. It is therefore reasonable to expect that the distribution equation will apply before, at, and very close beyond the critical point. The trend of Table I confirms this expectation. The nearer to the gel point, the closer the agreement between experiment and theory should be, and indeed is. In addition, the greater the size of the x-mer, the more pronounced the effects of entrapment and diffusion should be on a weight fraction basis (the effect becoming increasingly important at higher conversions). A monomeric or dimeric molecule is much more mobile than a pentadecameric molecule. In a rigid polymer network, the monomers and dimers should suffer least the consequences of diffusion and entrapment on their reaction fates and mobilities. A pentadecamer, however, would likely be seriously affected by such conditions. Thus, while the first and second solutions of the distribution expression give a fair fit to the experimental results, the fifteenth solution shows serious discrepancies.

In addition to the quantitative discussion related to the information in Figure 1, certain qualitative observations can be made, giving a clear demonstration of how the higher molecular weight species are preferentially attached to the gel phase. The long high molecular weight tail present in the sol fraction of $p = 0.726$ apparently confers a highly skewed shape on the chromatogram. The detection of material of molecular weight as high as 5×10^6 (Figure 4 for $p = 0.726$) also confirms that the continuous light-scattering response of Figure 1 (for the same sample) is real and not an instrumental artifact. It is the material under this high molecular weight tail that is first consumed in building the network. An increase of about 4% in the conversion parameter (from $p = 0.726$ to $p = 0.767$) results primarily in the consumption of this high molecular weight tail. It is predictable, therefore, that the weight fractions of the monomeric species within the sol monotonically increase beyond the gel point.

Figure 4 also shows that as the polymerization proceeds beyond the gel point, the number of species in the sol becomes progressively smaller. At $p = 0.877$, there are only a few species present with molecular weight greater than 10^3, a considerably simplified distribution compared to that of the sol at $p = 0.726$ (i.e., near the gel point). It is therefore reasonable to expect that at the limiting value of $p \rightarrow 1.0$, the number of species present in the sol will be only the starting monomers as depicted in the theoretical plot of Figure 2.

Experimental Section

Polymerization beyond the Gel Point. Predried 1,3,5-benzenetriacetic acid and decamethylene glycol were accurately weighed in exact stoichiometry (i.e., 2/3) in a polymerization tube. A small magnetic stirrer was introduced to facilitate mixing during the reaction.

The tube was sealed with a rubber septum, and dry nitrogen was passed in at a moderate rate to exclude oxygen. The needles used for the nitrogen inlet and outlet were removed, and the tube was immersed in an oil bath preset at 170 °C, heated by a hot plate with a magnetic stirring motor. Within 5 min the low-melting diol component had melted and the mixture was partly homogenized. Then the temperature was rapidly lowered to 155 °C by adding cold oil to the heating bath. At selected time intervals after gelation the tube was withdrawn and wiped clean. while the tube was still hot, its septum was removed, and it was placed in a vacuum desiccator (at $\simeq 10^{-3}$ mmHg) over KOH to reach room temperature. Finally, its surface was dried and degreased with acetone. The difference in weight was used to calculate the extent of reaction.

Sol Fraction Isolation, Clarification, and Analysis. In order to extract the soluble polymers at various extents of reaction beyond the gel point, the material within the polymerization tube was first allowed to swell in 10 mL of THF overnight. The swollen gel was then broken into small pieces by applying slight pressure on it with a long metallic spatula against the walls of the tube. Then the pulverized gel was extracted with fresh THF (usually 8×10 mL). The solvent was filtered through a fine porous funnel into a 150-mL predried, preweighed round-bottomed flask. Gels produced in the $0.720 \leq p \leq 0.795$ region were found to swell extensively. Since this property made them difficult to wash free of sol through a porous funnel, the sol was recovered quantitatively by washing the gel in centrifuge tubes. After centrifugation, the supernatant liquid was carefully withdrawn and filtered through a porous funnel into an appropriate flask. After 8–10 such washings the gel was quantitatively transferred to a filter paper cone and thoroughly washed with solvent. The collected washings, after further filtration through the porous funnel filter, were combined with the original extract, and the solvent was evaporated under reduced pressure at 40 °C.

The soluble fraction from each experiment thus isolated was clarified as follows. Each sample was redissolved in distilled, peroxide-free THF to give approximately 2% solution, and each solution was centrifuged at $27 \times 10^3 g$ for 1 h. The supernatant

liquor was carefully withdrawn, and the residue was washed with 5 mL of THF and recentrifuged. Washing and centrifuging were repeated three times. The combined washings were evaporated at 40 °C and the sol was dried under high vacuum (10^{-3} mmHg) over KOH to constant weight.

The composite GPC/LALLS chromatograms reported were produced by injecting 250–500 μL of approximately 1–2% (w/v) (accurately known) THF sample solutions into a KMX-6 GPC/LALLS photometer instrument. Six μStyragel (Waters Associates) columns (10^5, 10^4, 10^3, 500, 10^6, and 100 Å) were used in the size exclusion process prior to the RI and LALLS detection. The flow rate of the effluent (THF) was always kept at 1 mL/min, and the anode sensitivity of the photomultiplier tube of the LALLS photometer was kept at a uniform 900-mV value.

In each set of runs reported, attempts were made to keep all experimental variables constant from sample to sample so that the resulting chromatograms would be comparable.

Acknowledgment. We thank Professor Walter H. Stockmayer for constructive criticism during review of our manuscript. The valuable contribution of Robert Poole of the Computing Section of the Pulp and Paper Research Institute of Canada also deserves our grateful acknowledgment.

Appendix

Stockmayer[7] in section IV of his paper theoretically examined the polyesterification of an f-functional monomer with two different difunctional monomers. The case under discussion in this work can be treated with these equations after certain simplifications.

According to the Stockmayer notation, n is the number of f-functional molecules within an x-mer, l is the number of difunctional molecules bearing functional groups A within an x-mer, and s is the number of difunctional molecules bearing functional groups B within an x-mer. For the simpler case of BTA/DMG, $\eta = 0$ and $l = 0$, thus the distribution law of eq 48 in Stockmayer's paper becomes

$$m_{n,s} = (A w_{n,s} \xi^n \zeta^s)/(n!s!) \tag{4}$$

where $m_{n,s}$ is the number of n,s-mers.

The Langrarian multipliers A, ξ, and ζ in expression 4 are given by Stockmayer in the set of equations numbered as (53). For our case, however, $\rho = 1$ and thus $\alpha = p^2$. The factor $w_{n,s}$ can also be evaluated from eq 49 in Stockmayer's work, once again by setting $l = 0$ and $q = s - n + 1$.

After the appropriate substitutions and rearrangements one may arrive at relation 5 for $m_{n,s}$, which is expressed in terms of known quantities. (A is simplified at the end of the procedure.)

$$m_{n,s} = \left(A \left[\frac{2^s f^n (fn - n)!s!}{(fn - n - s + 1)!(s - n + 1)!} \right] \times \left[\frac{pr(1-p)^{f-1}}{f(1-rp)} \right]^n \left[\frac{p(1-rp)}{2(1-p)} \right]^s \right) \Big/ (n!s!) \tag{5}$$

The weight fraction of any x-mer ($W_{n,s}$) within the polymerizing material can be expressed as follows:

$$W_{n,s} = \frac{nm_{n,s} + sm_{n,s}}{N + S} \tag{6}$$

where N and S are the number of f-functional and bifunctional units in the system, respectively. Once again they can be expressed in terms of known quantities from the ratios N/A and S/A given by the set of equations numbered (50) in the Stockmayer paper. After another set of substitutions and rearrangements, one arrives at eq 2.

The condition for the lowest number of f-functional units in a given $(n + s)$-meric chain is given by

$$\text{lowest number of } f\text{-functional units} \geq [(n + s) - 1]/f$$

For example, for $n + s = 15$, the lowest number of trifunctional units $\simeq 5$ and the lowest number of difunctional units = 7. As such, the following solutions of eq 2 are needed in order to evaluate $W_{x=15}$, which is the sum of these: $n = 5$, $s = 10$; $n = 6$, $s = 9$; $n = 7$, $s = 8$; $n = 8$, $s = 7$.

In deriving theoretical values of W_x from eq 1, the following approximations are required: $f = 2.5$ and $\alpha = p$. The fractional factorials thus appearing in the expression can be calculated from the following Γ function, which is known to approximate the solution to a fourth decimal.

$$\Gamma(z) \sim e^{-z} z^{z-1/2} (2\pi)^{1/2} \left[1 + \frac{1}{12z} + \frac{1}{288z^2} - \frac{139}{51840z^3} - \frac{571}{2488320z^4} + \dots \right]$$

where z is (the fractional factorial to be evaluated + 1).

Registry No. BTA, 4435-67-0; DMG, 112-47-0; (BTA)(DMG) (copolymer), 34606-50-3.

References and Notes

(1) Flory, P. J. *Principles of Polymer Chemistry*; Cornell University Press: Ithaca, NY, 1953; Chapters IX and XIV. *J. Am. Chem. Soc.* **1941**, *63*, 3091.
(2) Burchard, W.; Kajiwara, K.; Gordon, M.; Kalal, J.; Kennedy, J. W. *Macromolecules* **1973**, *6*(4), 642.
(3) Peniche-Covas, C. A. L.; Gordon, M.; Judd, M.; Kajiwara, K. *Discuss. Faraday Soc.* **1974**, *57*, 165.
(4) Clarke, N. S.; Devoy, C. J.; Gordon, M. *Br. Polym. J.* **1971**, *3*, 194.
(5) Berry, R. M. Ph.D. Thesis, McGill University, Montreal, 1980.
(6) Falk, M.; Thomas, R. E. *Can. J. Chem.* **1974**, *52*, 3285.
(7) Stockmayer, W. H. *J. Chem. Phys.* **1943**, *11*, 45.
(8) Stockmayer, W. H. *J. Chem. Phys.* **1944**, *12*, 125.
(9) Macosko, C. W.; Miller, D. R. *Macromolecules* **1976**, *9*, 199, 206; **1978**, *11*, 656.
(10) Argyropoulos, D. S.; Bolker, H. I., to appear in *Makromol. Chem.*
(11) Kalal, J.; Gordon, M.; Devoy, C. *Makromol. Chem.* **1972**, *152*, 233.
(12) Chromatix Application Notes LS 1–6, Chromatix Inc. Sunnyvale, CA.
(13) Love, A. J. Ph.D. Thesis, Strathclyde University, 1968.
(14) Ross-Murphy, S. B. Ph.D. Thesis, Essex University, 1974.
(15) Argyropoulos, D. S.; Bolker, H. I., to appear in *J. Polym. Sci., Polym. Phys. Ed.*
(16) Argyropoulos, D. S.; Bolker, H. I. *Ind. Eng. Chem. Prod. Res. Dev.* **1986**, *25*, 575.
(17) Gordon, M.; Roe, J. *J. Polym. Sci.* **1976**, *21*, 75.